

Determining the Electronic Properties of Individual Nanointerfaces by Combining Intermittent AFM Imaging and Contact Spectroscopy

Ramsey A. Kraya, *Student Member, IEEE*, and Dawn A. Bonnell

Abstract—A method to determine the electronic properties at nanointerfaces or of nanostructures by utilizing intermittent contact atomic force microscopy and contact spectroscopy in one system is developed. By combining these two methods, the integrity of the interface or structure is maintained during imaging, while the extraction of the electronic information is obtained with contact spectroscopy. This method is especially vital for understanding interfaces between metal nanoparticles and substrates, where the nanoparticles are not tethered to the surface and can be combined with new and evolving techniques of thermal drift compensation to allow for a larger range of experiments on nanointerfaces and nanostructures in ambient environments. An experimental probe for quantifying the properties of individual interfaces with diameters in the range of 20 to 100 nm is developed, which is based on scanning probe microscopy.

Index Terms—Atomic force microscopy, metal nanoparticles, nanotechnology, semiconductor–metal interfaces, thermionic emission, transport.

I. INTRODUCTION

THE ABILITY to experimentally determine the electronic structure of nanointerfaces using atomic force microscope (AFM) techniques is of utmost importance to the advancement of nanointerface-controlled electronic devices. Interfaces in nanoscale devices may be an important component of the overall device function. However, it is not clear that the properties of nanoscale interfaces will be the same as those with macroscopic dimensions. Some observations indicate that interface properties will be size-dependent [1]. To understand the role of nanosized contacts in electronic devices, direct measurement of the properties of individual small interfaces is required.

To date, traditional methods of scanning probe microscopy, such as scanning tunneling microscopy (STM), contact atomic force microscopy, and impedance microscopy and spectroscopy

have been used to understand such interfaces [1]–[7]. However, it is extremely difficult to image metal nanoparticles and other nanostructures with these methods if the structures are not tethered to the surface. Attractive dielectrophoretic and image forces between a biased metal tip and metal nanoparticles have made STM an unsuitable method for imaging metal nanoparticles on substrate surfaces. These forces can overcome the adhesion of the particles to the surface causing the nanoparticles to jump and stick to the STM tip [8]. Similarly, contact AFM has proven as an ineffective technique for imaging most nanoparticles due to the fact that the probe itself moves the particle from the image window [9].

In intermittent contact AFM, the vibrating cantilever tip is brought close to the sample and for most of the oscillation period, the tip is not interacting strongly with the sample. The amplitude of the cantilever oscillation changes in response to tip-to-sample separation and is used for feedback of the vertical position of the AFM tip. This technique has proven valuable for imaging nanorods, nanoparticles, and delicate materials, due to the fact that the tip makes minimal contact with the sample, in contrast to contact-mode AFM imaging techniques. However, to characterize the properties of the interfaces, it is necessary to make and maintain constant mechanical contact and perform a range of electrical measurements in a manner that is not available in commercial instrumentation. Intermittent AFM imaging technique is usually coupled with force-distance spectroscopy, where the tip continuously cycles from a distance above the sample to contact, precluding electrical characterization.

Herein, the development of a control system is reported that incorporates contact electronic spectroscopy with intermittent contact AFM. This system protects the integrity of the sample during imaging and provides information on the electronic structure of interfaces and nanostructure and can be combined with new and evolving techniques of thermal drift compensation [10], [11] to allow for a larger range of experiments on nanointerfaces and nanostructures in ambient environments. We also report here an approach for fabricating nanosized metal–semiconducting oxide interfaces as models for examining contact properties. Interfaces fabricated in this manner are shown to exhibit ideal Schottky behavior and act as model interface systems.

II. EXPERIMENTAL PROCEDURES

A. System Design

The schematic diagram of the control system is shown in Fig. 1. A commercial AFM (Veeco Dimension 3100), three

Manuscript received July 8, 2009; revised January 24, 2010; accepted March 23, 2010. Date of publication March 29, 2010; date of current version November 10, 2010. This work was supported in part by the U.S. Department of Energy under Grant DE-FG02-00ER45813-A000, in part by the National Science Foundation Integrative Graduate Education and Research Traineeship (IGERT), in part by the Nano/Bio Interface Center under Grant IGERT DGE02-21664, and in part by the Laboratory for Research on the Structure of Matter under Grant DMR05-20020. The review of this paper was arranged by Associate Editor K. Wang.

The authors are with the Department of Materials Science and Engineering, University of Pennsylvania, Philadelphia, PA 19104 USA (e-mail: ramsey2@seas.upenn.edu; bonnell@lrsn.upenn.edu).

Color versions of one or more of the figures in this paper are available online at <http://ieeexplore.ieee.org>.

Digital Object Identifier 10.1109/TNANO.2010.2047024

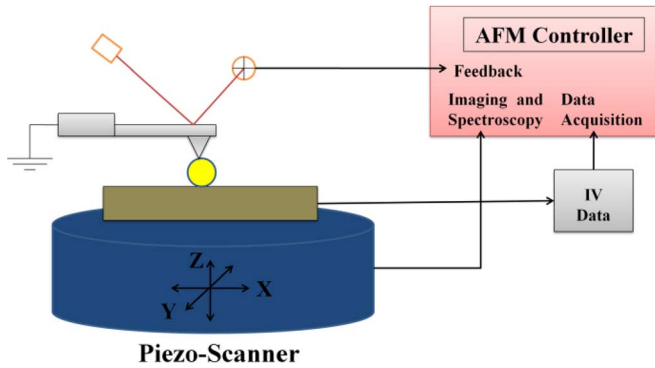


Fig. 1. Schematic diagram of a control system for combined intermittent contact imaging and contact spectroscopy. Feedback during imaging is based on the oscillation amplitude of the tip. For spectroscopic studies of the sample, the vertical deflection of the tip is used for feedback and the electronic structure is extracted.

power supplies, one oscilloscope, and a home-built switch circuit, are combined into an integrated control system. One power supply (an Agilent N6761A) with a voltage range of 0–50 V is used to supply voltage to the z-piezo during spectroscopy. The two power supplies ($2 \times$ N6734B) are connected in series to supply bias voltages between -10 to 10 V between the sample and AFM tip. The voltages from the commercial controller, which normally control the z-piezo are redirected to a two input switch box (PMII Computer Multiport Data Switch), whose output is connected to the z-piezo. The N6761A power supply is connected to the second input of the switch box. The oscilloscope (Tektronix DPO 4034) is used to measure the vertical deflection of the cantilever tip and the current directly from the microscope. Control of the system during spectroscopy is maintained by a MATLAB (version 2007b) program.

The sample is mounted on the AFM sample stage and the hood is closed on the system for a period of 12–24 h to reduce thermal drift to the order of 3–5 nm/min in both the x - and y -direction. Thermal drift correction software and a closed-loop AFM head are used to overcome any issues associated with imaging in ambient environments. Thermal drift can be overcome to the point that successive images of a 100 nm nanoparticle over a period of 30 min show no noticeable movement of the nanoparticle in a $1 \mu\text{m}$ image window. The closed-loop AFM head is used to position the tip at a location with an error no greater than a few nanometers.

While imaging, the AFM controller supplies the necessary voltage to the z-piezo. The AFM tips (Nanosensors, Inc.) are Pt/Ir coated silicon tips with a spring constant of 44 N/m and a resonant frequency of 171 kHz. Once a nanoparticle or structure has been located, the probe tip is positioned over the nanoparticle, the tip scan rate is reduced to zero and the drive voltages, which have been used to oscillate the tip are set to zero. The switchbox is then used to transfer control of the z-piezo from the AFM controller to the custom controller. The tip is lowered at a constant rate, and tip deflection is measured and is used as feedback. Once the desired deflection of the cantilever is achieved indicating contact with the surface, the voltage on the z-piezo is held constant. The sample bias (applied with the

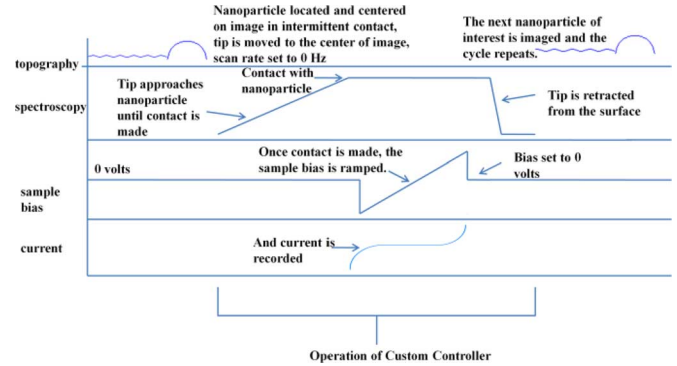


Fig. 2. Operation time-line of imaging and spectroscopy control system.

2N6734B power supplies) is step ramped over a range of ± 10 V at 1 V/s, accounting for the bandwidth of the preamplifier. The gain of the preamp is 10 pA/V with a maximum output voltage of 10 V. The current is recorded from the oscilloscope at each voltage step. Once the current–voltage data have been collected, the sample bias is set to zero volts and the tip is raised to its original position. Control of the z-piezo is transferred back to the AFM for normal imaging. Fig. 2 provides a timeline of the control system operation.

It is important to note that a bias between the sample and the tip is not applied until the tip has made contact to the nanoparticle and is removed before lifting the tip from the surface to avoid issues of attraction between the nanoparticles and the tip. If image and dielectrophoretic forces are not of concern, then feedback can be based on current instead of deflection, which would result in a gentler contact.

B. Fabrication and Testing

Interfaces were fabricated with colloidal gold nanoparticles on semiconducting SrTiO_3 substrates. A semiconducting oxide is chosen to facilitate experiments in ambient conditions without concern for difficulties due to oxidation. Similarly, a noble metal is used to avoid issues related to metal surface reaction. Single crystal, single-side polished, SrTiO_3 (100) doped with 0.2 at% Nb ($\text{SrTiO}_3\text{:Nb 0.2 at\%}$) and a geometry of $10 \times 5 \times 0.5 \text{ mm}^3$ were obtained from Princeton Scientific. The charge carrier density is $n = 9.8 \times 10^{18} \text{ cm}^{-3}$ assuming completely and singly ionized Nb-donors. The samples were cut with a diamond pen into sizes of $3 \times 3 \times 0.5 \text{ mm}^3$. The substrates were cleaned in ultrahigh purity (UHP) acetone for 1 min in an ultrasonic bath followed by a cleaning in UHP ethanol for 1 min. The substrates were then dried with a nitrogen gun followed by an annealing in oxygen at 1000°C for 1 h to remove oxygen vacancies and produce atomically smooth surfaces.

Gold colloids, obtained from British Biocell, are stabilized with a citrate shell and are suspended in an aqueous solution. A number of nanoparticle deposition techniques were attempted with the goal of depositing isolated metal nanoparticles of sufficient density for imaging within the scan range of an AFM. Boiling-on-contact was the most successful in terms of distribution and sample quality [12]. In this method, the SrTiO_3

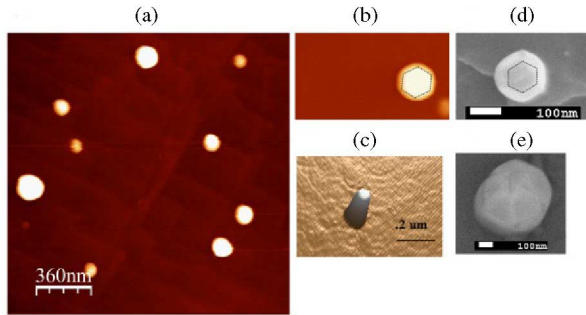


Fig. 3. (a) Topographic AFM image acquired of isolated gold nanoparticles on an atomically smooth SrTiO₃ $\langle 100 \rangle$ surface. Crystallographic steps on the substrate are along $\langle 100 \rangle$ directions. Renormalized contrast (b) and (c) show that the nanoparticles are truncated octahedron with the hexagonal surface in contact with the substrate. (d) SEM image of truncated octahedral gold nanoparticle on highly ordered pyrolytic graphite (HOPG) surface. (e) SEM image of truncated octahedral gold nanoparticle on 0.2 at% Nb-doped strontium titanate with the square face shown up.

substrate is placed on a hot plate and allowed to heat to a temperature of 350 °C for 10 min. The nanoparticle solution is then drop cast onto the SrTiO₃ surface, where the liquid solution evaporates immediately. Many “clean” areas are observed with only isolated nanoparticles visible on surface. In most areas, no salts are observed. The samples are then annealed in oxygen for 1 h at 950 °C to create a strong contact between the SrTiO₃ and the gold nanoparticles, remove the citrate shell from the nanoparticles, and control the morphology of the nanoparticles (see Fig. 3). Note that each metal particle is a single crystal.

The processing described earlier achieves the goal of isolated single crystal nanoparticle contacts with multiple well-controlled sizes on a single substrate. Fig. 3(a) shows a typical distribution of 20, 50, and 100 nm particles on a SrTiO₃ $\langle 100 \rangle$ surface. Note that the steps along $\langle 100 \rangle$ directions on the substrate, indicating that the surface is atomically smooth. Final annealing allows the nanoparticles to adopt surface energy driven morphology, which for gold is a truncated octahedral with $\langle 100 \rangle$ and $\langle 111 \rangle$ surface planes [13]. In this configuration, the interfaces are of SrTiO₃ $\langle 100 \rangle$ /Au $\langle 100 \rangle$, or SrTiO₃ $\langle 100 \rangle$ /Au $\langle 111 \rangle$ orientations with undetermined in-plane misorientation. The shapes of the particles are confirmed in SEM, but are also evident in AFM images, along with the expected tip convolution in the image [see Fig. 3(b) and (c)].

As noted earlier, previous attempts to image the nanoparticles using both STM and contact AFM faced significant challenges, however, this integrated control system was successful in both imaging and controlled contact with the nanoparticles. This control is illustrated in Fig. 4 in which imaging left three nanoparticles undisturbed [see Fig. (4a)], then a large load (~ 900 nN) was used to contact a nanoparticle of interest in a manner that allowed it to be removed from the surface, leaving the remaining nanoparticles undisturbed.

The properties of the Au nanoparticle–substrate interfaces are compared to those of a gold AFM tip–substrate contact in Fig. 5. The measured spring constant of the Au AFM tip was 44 N/m. In all cases, the Au nanoparticle–substrate interfaces exhibit ideal Schottky diode behavior with a turn-ON bias of 0.5–0.7 V and an

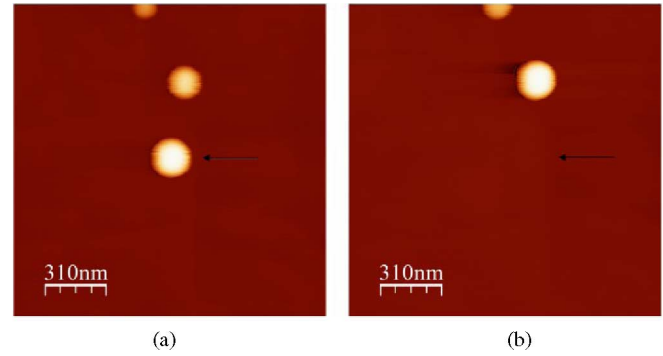


Fig. 4. AFM image before (a) and after (b) picking up just one nanoparticle from the surface using the custom controller.

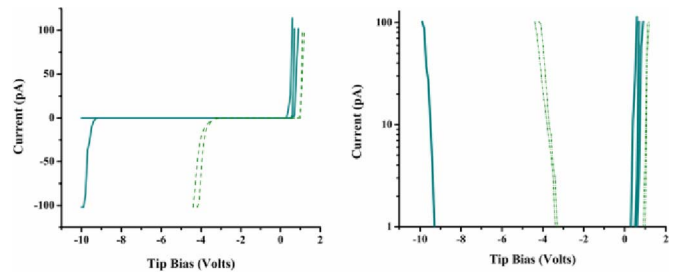


Fig. 5. Comparison of electronic properties of several Au nanoparticle–SrTiO₃ interfaces (solid lines) and tip–substrate contacts (dotted lines) on both linear (a) and log (b) scales acquired with custom control modification through an AFM tip.

absence of leakage current to high-reverse bias values. Three of the four interfaces resulted in no measureable leakage current to the maximum (-10 V), while one exhibited breakdown at -9.4 V. A Au tip–substrate contact interface results in a rectified I/V curve, with current at much lower reverse bias voltages.

To compare relative interface properties of the nanosized contacts, the barrier heights and ideality factors are estimated using classic thermionic emission theory. It has been shown that thermionic emission is a good description of transport across metal/SrTiO₃ interfaces. Current across an intimate, abrupt Schottky contact is described as follows:

$$I = AA^{**}T^2 \exp\left(-\frac{e\Phi^{\text{eff}}}{kT}\right) \exp\left(\frac{eV_D}{nk_B T}\right) \quad (1)$$

where A is the diode area, A^{**} is the effective Richardson constant, h is Planck’s constant, k is Boltzmann’s constant, V_D is the applied voltage, and Φ^{eff} is the effective barrier height. Using a least-squares fit to the data in Fig. 5, the barrier height and ideality factor of the interface between the 100 nm nanoparticles and SrTiO₃ substrate correspond to two values: $\Phi^{\text{eff}} = 0.6$ eV, $n = 2.8$ and $\Phi^{\text{eff}} = 1.0$ eV, $n = 1.1$. Since there are two sets of parameters and two orientations, the difference are attributed to the differences in the orientation and would suggest one orientation favors thermionic emission, while the other has a large tunneling component. It has been shown that SrTiO₃ can exhibit multiple simultaneous transport mechanisms (6) and the ratio is influenced by fields induced at the interface. Future studies will quantitatively address these transport mechanisms in nano

metal–semiconductor contacts. For the interface between the gold AFM tip and the SrTiO₃, which consists of an uncontrolled and unknown interface, $\Phi^{\text{eff}} = 1.3$ eV and $n = 1.3$.

These properties are in the same range as those reported earlier [14]–[18]. In the cases of the macroscopic electrodes and the AFM tip–substrate contact, the structure of the interface is random. The more controlled interfaces will allow properties to be related to interface structure and size. Perhaps more important, with direct measurements of individual nanocontacts, properties no longer need to be estimated from observations on large interfaces.

III. CONCLUSION

We have developed a new system and protocol for physically contacting nanosized interfaces without damage and demonstrated that it is successful even when the interfaces are weakly bound. An approach to making structurally controlled metal-oxide interfaces by exploiting the surface energy of metal nanoparticles and oxide substrates has been demonstrated. The electronic properties of model Schottky barrier contact at small scales have been quantified. This combination of imaging and contact spectroscopy enables reproducible electrical characterization of interfaces down to 20 nm diameters and can easily be extended to probe impedance, frequency dependence, and optoelectronic properties.

ACKNOWLEDGMENT

The authors would like to thank Dr. J. Santiago for helpful discussions.

REFERENCES

- [1] D. L. Carroll, M. Wagner, M. Ruhle, and D. A. Bonnell, "Schottky-barrier formation at nanoscale metal-oxide interfaces," *Phys. Rev. B*, vol. 55, pp. 9792–9799, 1997.
- [2] M. Sitti and H. Hashimoto, in *Proc. Int. Conf. Adv. Int. Mech.*, 1999, pp. 13–20.
- [3] T. Junno, S. Anand, K. Deppert, L. Montelius, and L. Samuelson, "Contact mode atomic-force microscopy imaging of nanometer-sized particles," *Appl. Phys. Lett.*, vol. 66, pp. 3295–3297, 1995.
- [4] D. A. Bonnell, Y. Liang, M. Wagner, D. Carroll, and M. Ruhle, "Effect of size dependent interface properties on stability of metal clusters on ceramic substrates," *Acta Mater.*, vol. 46, pp. 2263–2270, 1998.
- [5] R. Shao, S. V. Kalinin, and D. A. Bonnell, "Local impedance imaging and spectroscopy of polycrystalline ZnO using contact atomic force microscopy," *Appl. Phys. Lett.*, vol. 12, pp. 1869–1871, 2003.
- [6] S. V. Kalinin, D. A. Bonnell, M. Freitag, and A. T. Johnson, "Tip-gating effect in scanning impedance microscopy of nanoelectronic devices," *Appl. Phys. Lett.*, vol. 27, pp. 5219–5221, 2002.
- [7] S. V. Kalinin, M. R. Suchomel, P. K. Davies, and D. A. Bonnell, "Potential and impedance imaging of polycrystalline BiFeO₃ ceramics," *J. Amer. Cer. Soc.*, vol. 85, pp. 3011–3017, 2002.
- [8] J. Grobleny, D.-H. Tsai, D.-I. Kim, N. Pradeep, R. F. Cook, and M. R. Zachariah, "Mechanism of nanoparticle manipulation by scanning tunnelling microscopy," *Nanotechnology*, vol. 17, pp. 5519–5524, 2006.
- [9] T. Junno, S. Anand, K. Deppert, L. Montelius, and L. Samuelson, "Contact mode atomic-force microscopy imaging of nanometer-sized particles," *Appl. Phys. Lett.*, vol. 66, pp. 3295–3297, 1995.
- [10] B. Mokaberi and A. Requicha, *IEEE Trans. Autom. Sci. Eng.*, vol. 3, no. 3, pp. 199–207, Jul. 2006.
- [11] M. Abe, Y. Sugimoto, T. Namikawa, K. Morita, N. Oyabu, and S. Morita, "Drift-compensated data acquisition performed at room temperature with frequency modulation atomic force microscopy," *Appl. Phys. Lett.*, vol. 90, pp. 203103-1–203103-3, 2007.
- [12] K. Lee, M. Duchamp, G. Kulik, A. Magrex, J. Won Seo, S. Jeney, A. J. Kulik, L. Forro, R. S. Sundaram, and J. Brugger, "Uniformly dispersed deposition of colloidal nanoparticles and nanowires by boiling," *Appl. Phys. Lett.*, vol. 91, 2007.
- [13] J. H. Shim, B. J. Lee, and Y. W. Cho, *Surf. Sci.*, vol. 512, pp. 262–268, 2002.
- [14] T. Shimizu, N. Gotoh, N. Shinozaki, and H. Okushi, "The properties of Schottky junctions on Nb-doped SrTiO₃ (001)," *Appl. Surf. Sci.*, vol. 117, pp. 400–405, 1997.
- [15] M. Copel, P. R. Duncombe, D. A. Neumayer, T. M. Shaw, and R. M. Tromp, "Metallization induced band bending of SrTiO₃ (100) and Ba_{0.7}Sr_{0.3}TiO₃," *Appl. Phys. Lett.*, vol. 70, pp. 3227–3229, 1997.
- [16] R. Schafrank, S. Payan, M. Maglione, and A. Klein, "Barrier height at (Ba,Sr)TiO₃/Pt interfaces studied by photoemission," *Phys. Rev. B*, vol. 77, 2008.
- [17] T. Shimizu and H. Okushi, "The properties of a metal-oxide-semiconductor junction prepared using a high-purity ozone surface-treatment," *Appl. Phys. Lett.*, vol. 67, pp. 1411–1413, 1995.
- [18] A. Inoue, K. Izumisawa, and H. Uwe, *Jpn. J. Appl. Phys.*, vol. 40, pp. 3153–3156, 2001.

Ramsey A. Kraya (S'02) received the Bachelor's degree in electrical engineering, in 2004, the M.Sc. degree in electrical and computer engineering, in 2005, from the University of Delaware, Newark, DE, and the M.Sc. in materials science and engineering from the University of Pennsylvania, Philadelphia, in 2006, where he is currently working toward the Ph.D. degree.

He was an Employee of Conectiv Power Delivery, the American Competitiveness Institute, and Promenix Inc. on projects ranging from software development to hardware design.

Mr. Kraya is member of Eta Kappa Nu, Tau Beta Pi, the Materials Research Society, the Penn Energy Group. He is a Director for the Penn Biotechnology Group. He was the recipient of the IEEE Delaware Bay Award in 2004 and the National Science Foundation Integrative Graduate Education and Research Traineeship Fellowship in 2006.

Dawn A. Bonnell, photograph and biography not available at the time of publication.